HIGH-FREQUENCY ACOUSTIC SCATTERING AND ABSORPTION EFFECTS WITHIN SHIP WAKES

M. TREVORROW

Defence R&D Canada Atlantic, 9 Grove St., Dartmouth, Nova Scotia, Canada
E-mail: mark.trevorrow@drdc-rddc.gc.ca

Clouds of small air-bubbles injected and mixed into the near-surface ocean within vessel wakes can create significant acoustic scattering and extinction. Recent high frequency (100 kHz) sidescan sonar measurements on a moving vessel showed persistent strong backscatter features and significant dropouts in sea-surface reverberation behind the wakes. Details of the sonar measurements and features of ship wakes recorded during these sonar trials are reviewed. Estimates of typical wake width, persistence, backscatter strength, and effective extinction are presented for the case of straight-running and turning vessels at speeds up to 20 knots.

1 Introduction

Surface ship wakes are a significant underwater acoustic feature due to the injection of clouds of small air-bubbles, with their accompanying backscatter and extinction properties. These bubbles are created by propeller cavitation, breaking of the ship's bow and stern waves, and air entrainment in the turbulent boundary layer around the hull. After initial injection, these bubbles are re-distributed by wake flows and turbulence and subject to buoyancy, coalescence, and dissolution processes, dissipating over periods of 10 to 15 minutes. Several previous studies [1-4] have documented the basic properties of ship wakes, wherein the bubbly wake penetrates to depths up to 2 times the ship's draft and spreads horizontally to widths up to 5 to 10 times the ship's beam. In addition to their obvious naval importance as a surface ship signature, wakes are ideal for testing models on bubble dynamics and high-frequency propagation in bubbly media [4,5].

This work describes results from a 100 kHz side-looking sonar sampling the wake of a maneuvering vessel from a distance of approximately 500 m. While previous studies have generally focused on vertical profiling within the wake, hence only sampling a limited volume, this work looks at the macroscopic features of the wake employing a relatively distant side-looking sonar in a surface-grazing geometry. This is the same geometry as would be used in an obstacle avoidance sonar from a ship or autonomous vehicle, where confusion of target ship and its wake needs to be addressed. Looking perpendicular to the wake yields a backscatter profile that initially widens and grows in strength as the wake deepens, then dissipates over a period of 10 to 15 minutes. A key feature of this geometry is that acoustic extinction in the near side of the wake affects sampling of farther regions. Overall, this wake study was undertaken to determine how wake backscattering is affected by vessel speed and maneuvers.

2 Observational Methods

The sea trials were conducted with a medium-sized, twin-propeller vessel in Bedford Basin, Nova Scotia on March 11th, 2004. The focal point of the trials was the DRDC Atlantic *Acoustic Calibration Barge* (ACB), where a 100 kHz sonar system was mounted. During the day, the ship performed a total of 24 pre-defined runs in the vicinity of the ACB at 10, 15 and 20 knots, with a 400 to 500 m closest point of approach (CPA). Three distinct types of runs were performed: straight-line, 90° turns, and full-circle turns (the turns were always *away* from the ACB). At or just prior to CPA the ship heading was nearly perpendicular to the sonar beams. These sonar measurements sought to quantify the scattering strength and persistence of the bubbly wake at various speeds and during maneuvers. The runs were conducted at least 15 minutes apart to allow the previous wake to drift away from the CPA and dissipate. Two differential GPS systems were installed on the vessel bow and stern near the vessel center-line, from which vessel speed and heading, and range and bearing from the sonars on the ACB, could be calculated. The wind conditions generally increased from 10 to 20 knots during the day, producing significant white-capping in the later runs. The water depth in the vicinity of the ACB was roughly 45 m.

This work utilized a four-channel, 100-kHz sidescan sonar system capable of operating up to 750 m slant range [6]. For these trials a simple 1 ms gated-CW pulse was used, providing 72-cm acoustic resolution. Each channel was coherently sampled at 20,000 samples per second, providing 3.7 cm sampling resolution, with 16-bit (92 dB) dynamic range. A time-varying gain was utilized to partially compensate for geometric spreading and absorption losses. Maximum sampling ranges between 600 and 750 m were utilized, allowing pulse repetition rates between 0.8 and 1.0 pings per second. The 100-kHz sidescan transducers had fan-shaped beams 3° x 60° (to -3 dB points), mounted with their wide (60°) beam apertures oriented vertically, with the main axes horizontal. The four transducers were oriented at approximately 5° azimuthal increments to provide a wider overall coverage area and slightly different incidence-angle looks at the vessel. The four transducers were mounted on a rotating calibration station at the ACB, oriented towards the vessel CPA. The transducer depth was 8.4 m. During these trials a lower-frequency (20 – 40 kHz) sonar was also operated from the ACB, occasionally inducing acoustic interference in the 100 kHz system. Attempts were made to filter out this cross-talk, with partial success.

The fact that these trials used a surface-grazing geometry at ranges up to 500 m suggested that acoustic propagation effects might be important. During the trials several sound velocity profiles were collected from the ACB, with conditions on March 11th showing a generally upward-refracting profile with a distinctly colder surface layer in the upper 2 m. A simple *ray-tracing* analysis was used to quantitatively predict the transmission loss from the source to the target, using the measured sound speed profile, a 500 m sonar-to-ship separation, and assuming a wake located in the upper 5 m. Two near-surface, refracted eigenrays were identified: a direct path and a singly surface-reflected ray. The modeling found that these two near-surface rays generally produced a 0.5 dB propagation enhancement relative to spherical spreading. However, it is believed that ambient bubble layer losses (from natural white-capping) would reduce the intensity of the surface-reflected ray, such that simple spherical spreading appears a reasonable assumption. Additionally, note that the relatively wide vertical aperture allows reception

of seabed backscatter beyond roughly 100 m range, which is responsible for some of the reverberation in vicinity of the vessel wakes.

Calibration of the high-frequency backscatter sonars was accomplished using echoes from a 0.914 m outside diameter, hollow steel sphere (6.4 mm shell thickness) moored approximately 250 m SE of the barge, approximately 3 m below the surface. Using well-known analytic models for spherical shell backscatter, the target strength (*TS*, 10 x common logarithm of the backscatter cross-section in m^2) was calculated as a function of frequency. The predicted sphere *TS* at 100 kHz, corrected for the finite band-width of the transmitted pulse (1 ms duration), was -11.5 dB (re m^2). This is similar to the *TS* predicted under a rigid body assumption of $10 \cdot \log_{10}[\text{radius}^2/4]$ = -12.82 dB.

The sphere echoes appeared as small but distinct intensity peaks near 245 m range. The transducer mounting was rotated manually until the target sphere echo (at known range and heading) appeared to have maximum intensity in one of the channels. Then ping data was recorded and averaged over 400 separate pings at a fixed sonar heading, and the process repeated for each of the four channels. Then, the total systemic calibration coefficient, *K*, for each channel was extracted through application of the standard sonar equation, specifically

$$K = TS_{\text{sphere}} - 20 \cdot \log_{10}[A_{rms}] - 2TL + TVG \qquad \text{(in dB)} \qquad (1)$$

where A_{rms} is the averaged sphere echo amplitude, *TL* is the acoustic transmission loss, given by the sum of spherical spreading ($20 \cdot \log_{10}$[range]) and an acoustic absorption term (α = 0.021 $dB \cdot m^{-1}$ at 100 kHz under these water conditions), and *TVG* is the time-varying gain. The sonar *TVG* was determined by averaging sonar data with the transmit power turned off. A re-arrangement of Eq.1, with an added term to account for the insonified volume of the sonar, is then used to calculate the estimated volumetric backscatter strength (described below).

3 Sidescan Sonar Observations

Although a variety of runs were performed, the contrast between straight-line and 90°-turning maneuvers at 20 knots is the most illuminating. Figures 1 and 2 present example wake images for these two cases. In the straight-line run (Fig. 1) echoes from the vessel hull can be seen following a hyperbolic trajectory centered on the CPA. Fig. 1 also shows an intense noise event (vertical line) coincident with the vessel mid-section passing through CPA, presumably due to propeller cavitation. The hull echo and noise line are less prominent in the 90°-turn image (Fig. 2), however some other similar turning runs do show such features clearly. Constant-range reverberation lines in both images are seabed echoes. Surface reverberation appears as cloudy, diffuse bands drifting slowly towards the sonar, more prominent in Fig. 2.

The straight-line run (Fig. 1) shows three distinct wake features: a central core beginning near the CPA and spreading to a width roughly equal to the ship beam over the first 250 s, an outer wake edge more rapidly expanding towards the sonar, and an inner wake line expanding to an intermediate across-track range. The central core is a typical feature of twin-screw vessels, and its relatively high intensity is presumably due to deeper bubble penetration in the central down-welling zone. The disappearance of the wake central core after time = 280 s has been noted previously by several

investigators [3,4], and is possibly due to higher concentrations of larger diameter bubbles which rise to the surface relatively quickly. The outer wake edge expands and intensifies to a define a wake half-width of roughly 4 ship beams by the right-hand edge of the image, some 480 s after passage of the vessel. Note that although this straight-line wake should be approximately symmetric about the CPA, the further side of the wake beyond CPA does not appear in the sonar image, either in the central core or the outer edge. This is presumably due to strong acoustic extinction effects in the near side and central core of the wake. Also, the apparent disappearance of the wake central core after time = 280 s may be partly attributable to this effect.

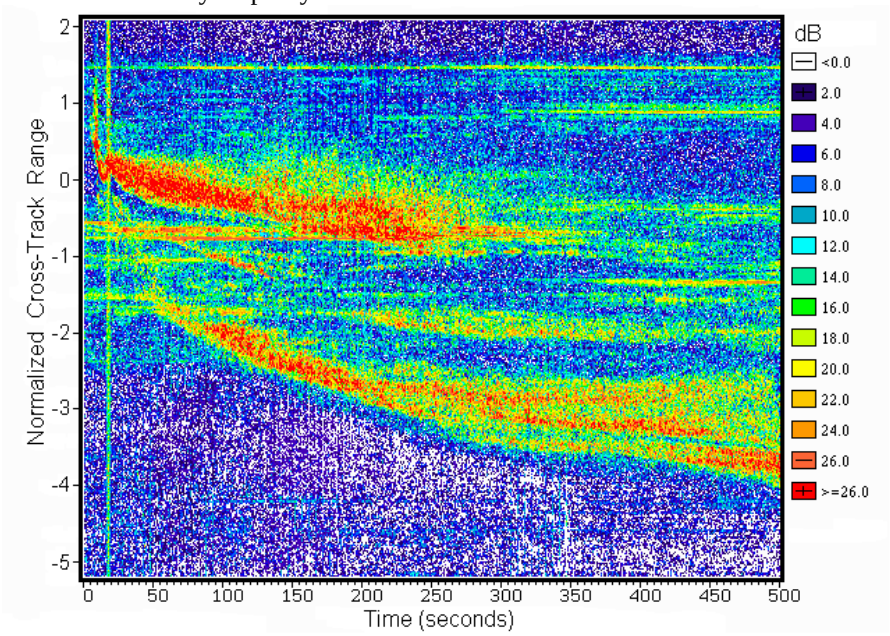

Figure 1 100 kHz sidescan intensity (arbitrary dB) vs. normalized cross-track range and time showing wake evolution for a straight-line run at 20 knots starting 1407UT, 11March 2004. Cross-track range relative to CPA and normalized by vessel beam.

A similar, yet stronger acoustic extinction effect appears in the 90°-turning run (Fig. 2), where the central core is only visible for roughly 100 s after CPA and there is a distinct signal drop-out at ranges beyond the outer wake edge at times >150 s. In this turning maneuver the wake outer edge now expands to at least 8.5 times the ship beam towards the sonar, and is much more intense in early portions of the wake formation. A characteristic of sharp turns with a vessel of this size is the creation of an overturning horizontal vortex as the vessel slides partly side-ways through the water [4,7]. This vortex rotates outward along the surface, creating a strong convergence and down-welling zone that migrates outwards from the turn, with a relatively smooth divergent surface region behind it. Similar to the straight-line run there are no wake features at ranges beyond CPA, although it should be noted that this wake is inherently asymmetric. Note a distinct drop-out in reverberation in behind the wake edge (cross-track range near -1 to -3 ship beams) beginning at roughly 150 s.

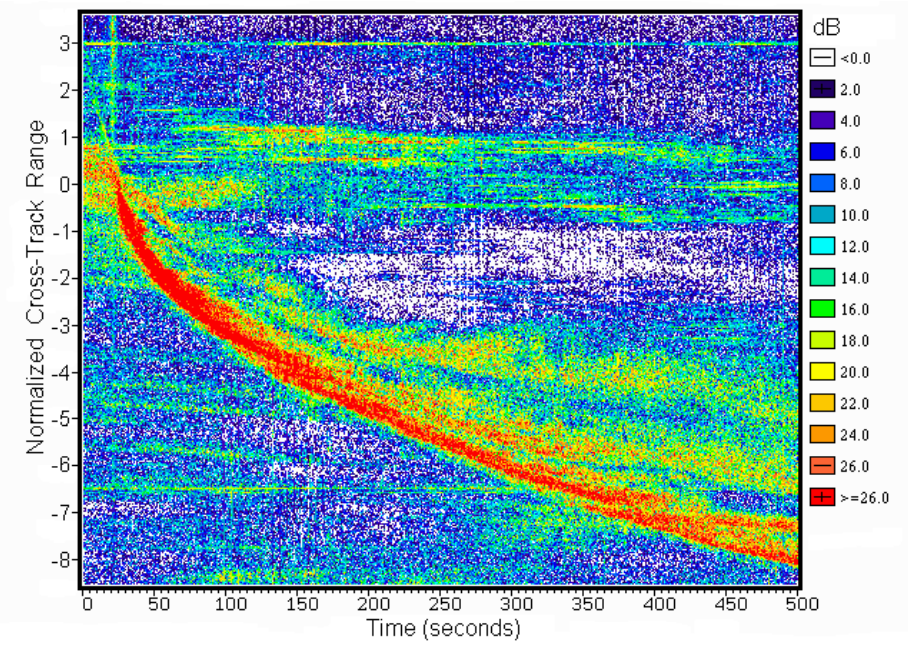

Figure 2 100 kHz sidescan intensity (arbitrary dB) vs. normalized cross-track range and time showing wake evolution for a 90°-turn run at 20 knots starting 1526UT, 11March 2004. Cross-track range relative to CPA and normalized by vessel beam.

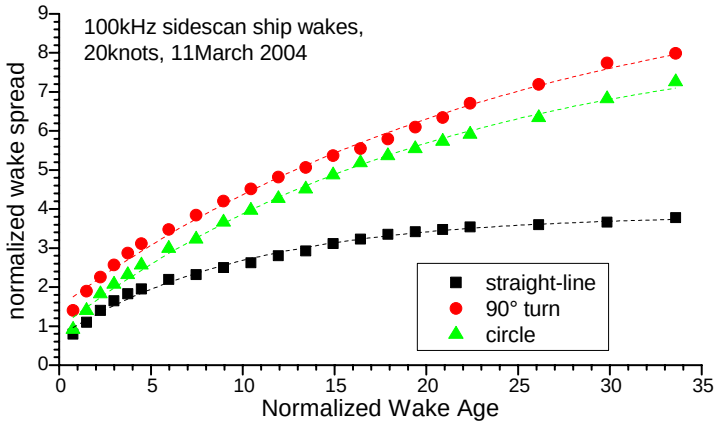

Figure 3 Comparison of normalized wake spread [(CPA – near_wake_edge) / beam] vs. wake age in ship-lengths for straight-line, 90°-turn, and full-circle wakes at 20 knots. Dashed lines show corresponding fitted curves of the form *width* = A[1 – B*exp(-t/t_0)].

The overall across-track spread of the wake can be extracted from these images, as summarized in Figure 3. Clearly, the outer wake edge in the two turning runs expands to roughly twice that observed for the straight-line run, with quantitatively similar behavior for the 90°-turn and full-circle maneuvers. Due to the expected symmetry of

the straight-line run this spread is one-half of the total width, and is consistent with wake width and time scales observed previously [3,4]. It is presumed that the turning-maneuver wakes show enhanced spreading due to greater horizontal migration of the overturning vortex. All three wakes show a time-evolution consistent with an exponential-decay approach to a maximal value, with time constants ranging from 137 s (straight-line) to 338 s (90° turn).

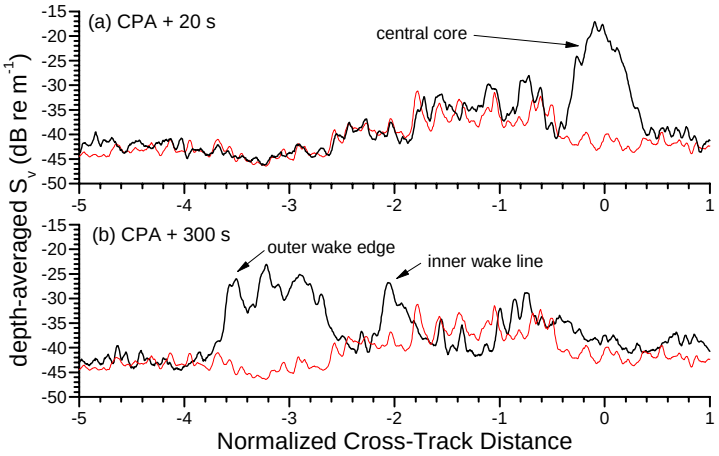

Figure 4 Profiles of averaged volumetric backscatter strength at two points in the wake evolution of the straight-line run at 20 knots (data shown in Fig. 1). Cross-track distance relative to CPA and normalized by vessel beam. (a) early wake 20 s after CPA, and (b) late wake 300 s after CPA. Both profiles averaged over 10 s (black line), and compared to background reverberation averaged over 30 s just prior to CPA (red line).

The sonar calibrations allow estimates of the apparent wake target strength and other acoustic characteristics. In this horizontal sonar geometry only depth-integrated wake backscatter can be extracted. From previous studies with vertically profiling echo-sounders [3,4] similar vessel wakes were found to have a roughly uniform volumetric scattering strength from the surface to 5 - 8 m depth. In this case we shall calculate a depth-averaged volumetric scattering strength, $\langle S_v \rangle$, assuming the total volume of wake insonified by the sonar is one ship draft in depth by 3.0° horizontal angle by 72 cm in range (one pulse-length). Cross-wake profiles for the two run types are shown in Figures 4 and 5. At a fixed sonar frequency and assuming a particular size distribution of the micro-bubbles, the total extinction cross-section, s_e, is proportional to the volumetric backscatter cross-section (linear equivalent of S_v) [8]. Specifically in the near-surface region at 100 kHz the ratio between extinction and backscatter cross-sections is approximately 60. Then the extra transmission loss due to bubbles is

$$TL_{bub} = 4.34 \int_{path} s_e \cdot dl \qquad \text{(in dB)} \qquad (2)$$

where l is distance along the acoustic path. Since the depth variation in s_e is not known, only averaged estimates of TL_{bub} can be produced. Furthermore, since some portion of the observed backscatter is due to seabed reverberation, which is not subject to wake extinction, it is not appropriate to blindly apply extinction corrections to the profiles.

Figures 4 and 5 show 10-s averaged profiles at two times in the wake evolution compared to the background reverberation prior to CPA. In Fig. 4a the early wake is dominated by the central core near CPA, with a $<S_v>$ reaching a maximum near -17.0 dB (re m^{-1}), more than 22 dB higher than the background. The remainder of the profile, being dominated by seabed reverberation, is largely unchanged. The one-way path-integrated bubble loss (Eq.2) across this wake core is 17.8 dB, or 35.6 dB for the two-way loss appropriate for backscattering. Clearly this extinction effect is responsible for the lack of wake signal beyond CPA, and a diminished scattering strength in the far side of the central core. At later times (Fig. 4b) the outer wake edge dominates, with $<S_v>$ averaged over -3.6 to -2.8 ship beams reaching -27.5 dB (re m^{-1}). This is again roughly 20 dB above the reverberation, with a two-way integrated bubble loss of 15.0 dB. In Fig. 4b the central core has either dissipated or been rendered invisible by extinction effects in the outer wake edge, or both.

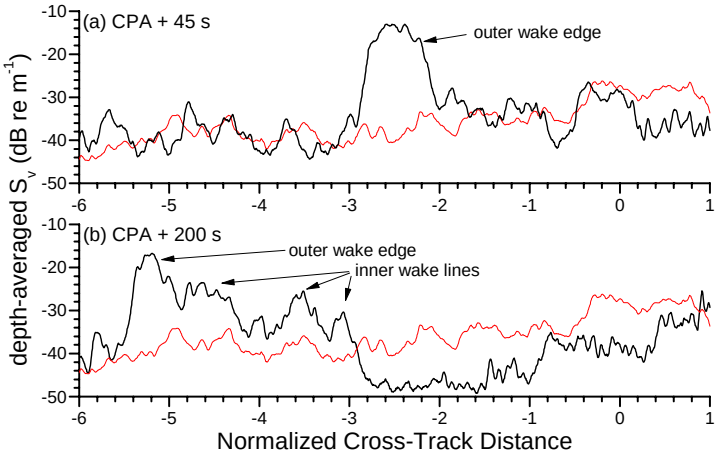

Figure 5 Profiles of averaged volumetric backscatter strength at two points in the wake evolution of the 90° turn run at 20 knots (data shown in Fig. 2). Cross-track distance relative to CPA and normalized by vessel beam. (a) early wake 45 s after CPA, and (b) later wake 200 s after CPA. Line definitions similar to Fig. 4.

In the 90° turning maneuver (Figure 5) the wake profiles are dominated by the outer wake edge almost immediately after CPA, with scattering strength and extinction much stronger than the straight-line run. In Fig. 5a the early wake formation is dominated by a strong outer wake edge centered at -2.5 ship beams with $<S_v>$ = -15.2 dB (re m^{-1}). This creates a bubbly region roughly 0.8 ship beams wide with a one-way integrated bubble loss of 89.8 dB. Clearly acoustic signals cannot penetrate such a feature. Even at later times (Fig. 5b) where the outer wake edge has spread and dispersed somewhat, the peak $<S_v>$ near -5.2 ship beams still reaches approximately -20 dB (re m^{-1}), with a one-way integrated bubble loss of 22.8 dB. In the later wake profile, there is a reverberation drop-out of roughly 5 to 10 dB at ranges from -3 to +1 ship beams, presumably due to acoustic extinction in the outer and inner wake lines. The remaining $<S_v>$ profile in this drop-out zone is composed of seabed reverberation and systemic noise contributions.

4 Concluding Remarks

When viewed in a horizontal, surface-grazing geometry at relatively high acoustic frequencies (>20 kHz), ship wakes are a significant acoustic target. These high-resolution sonars captured the evolution of a central core roughly one ship beam wide and several outer wake lines. Overall the wakes were observed to dissipate over 12 to 15 minutes, depending on the vessel speed and maneuvering state. At 20 knots the outer wake edge expanded to a half-width of 3.8 ship beams wide in a straight-line run, and expanded to more than 8.5 ship beams during a 90°-turning run. The stronger outer wake edge in the turning maneuvers is believed to be due to the creation of an overturning horizontal vortex as the vessel slides partly side-ways through the turn. This vortex rotates to the outside of the turn along the surface, creating a strong convergence and down-welling zone that migrates outwards, with a relatively smooth divergent surface region behind it. Similar vortex formation has been observed previously [4,7] in the case of straight-line runs. In general only minor differences were observed between 90°-turn and full-circle maneuvers. Assuming the wake to be roughly uniform up to 1 ship draft in depth, peak volumetric backscatter strengths exceeded –15 dB (re m^{-1}), with predicted one-way acoustic extinction losses in the range 15 to 90 dB. These extinction losses are presumed to be responsible for a lack of observed wake features at ranges beyond the CPA.

Acknowledgements

The author is grateful for the assistance of Art Collier and Boris Vasiliev of DRDC Atlantic for their assistance during the vessel trails. Dr. John Fawcett of DRDC Atlantic provided the spherical shell target strength calculations.

References

1. National Defense Research Committee Div. 6, Physics of Sound in the Sea, Summary Technical Report Volume 8, reprinted 1969 as NAVMAT Report P-9675 (original 1946).
2. Ezerskii, A., Sandler, B., and Selivanovskii, D., Echo-ranging observations of gas bubbles near the sea surface, *Sov. Phys. Acoust.* **35**(5), 483-485 (1989).
3. Trevorrow, M., Vagle, S., and Farmer, D., Acoustic measurements of micro-bubbles within ship wakes, *J. Acoust. Soc. Am.* **95**(4), 1922-1930 (1994).
4. Weber, T., Lyons, A., and Bradley, D., An estimate of the gas transfer rate from ocean bubbles derived from multibeam sonar observations of a ship wake, *J. Geophys. Res.* **110** (C04005) (2005).
5. Vagle, S., and Burch, H., Acoustic measurements of the sound speed profile in the bubbly wake formed by a small motor boat, *J. Acoust. Soc. Am* **117**(1), 153-163 (2005).
6. Trevorrow, M., and Myers, V., Description and evaluation of a four-channel, coherent, 100-kHz sidescan sonar, DRDC Atlantic Technical Memorandum 2004-204 (2004).
7. Marmorino, G., and Trump, C., Preliminary side-scan ADCP measurements across a ship's wake, *J. Atmos. Oceanic Tech.* **13**, 507-513 (1996).
8. Trevorrow, M., Measurement of near-surface bubble plumes in the open ocean with implications for high-frequency sonar performance, *J. Acoust. Soc. Am.* **114**(5), 2672-2684 (2003).